Hindawi
Advances in Civil Engineering
Volume 2020, Article ID 6958642, 14 pages
https://doi.org/10.1155/2020/6958642

Research Article

Laboratory Tests for Subgrade Reaction Coefficient in Seismic Design of Underground Engineering Domain

Kunpeng Xu,[1] Liping Jing ,[1] Xinjun Cheng,[2] Haian Liang,[2] and Jia Bin[3]

[1]*Key Laboratory of Earthquake Engineering and Engineering Vibration, China Earthquake Administration, Institute of Engineering Mechanics, China Earthquake Administration, Harbin 150080, Heilongjiang Province, China*
[2]*State Key Laboratory of Nuclear Resources and Environment, East China University of Technology, Nanchang 330013, Jiangxi Province, China*
[3]*College of Civil Engineering, Hunan University of Technology, Zhuzhou 412000, Hunan Province, China*

Correspondence should be addressed to Liping Jing; jlp_iem@163.com

Received 8 January 2020; Revised 3 May 2020; Accepted 11 June 2020; Published 28 June 2020

Academic Editor: Xiaodong Hu

Subgrade reaction coefficient is commonly considered as the primary challenge in simplified seismic design of underground structures. Carrying out test is the most reliable way to acquire this intrinsic soil property. Owing to the limitations of experimental cost, time consumption, soil deformation mode, size effect, and confined condition, the existing testing methods cannot satisfy the requirements of high-precision subgrade reaction coefficient in seismic design process of underground structures. Accordingly, the present study makes an attempt to provide new laboratory testing methods considering realistic seismic response of soil, based on shaking table test and quasistatic test. Conventional shaking table test for sandy free-field was performed, with the results indicating that the equivalent normal subgrade reaction coefficients derived from the experimental hysteretic curves are reasonable and verifying the deformation mode under seismic excitation. A novel multifunctional quasistatic pushover device was invented, which can simulate the most unfavorable deformation mode of soil during the earthquake. In addition, the first successful application of an innovative quasistatic testing method in evaluating subgrade reaction coefficient was reported. The findings of this study provide preliminary detailed insights into subgrade reaction coefficient evaluation which can benefit seismic design of underground structures.

1. Introduction

With the rapid development of urbanization process in China, underground structures are being increasingly constructed in recent years. These underground structures play a crucial role in the civil infrastructure domain and are subjected to natural risks including earthquake disaster during operation stage [1]. Underground structures are generally deemed to perform better than aboveground structures in seismic resistance; thus, it is not astonishing that the antiseismic design of underground engineering has been neglected until recent years. However, the damage to many important underground infrastructures during earthquake events, for instance, the Kobe earthquake in Japan (1995), the Chichi earthquake in Taiwan (1999), and the Wenchuan earthquake in China (2008), has supported the concept that underground engineering is vulnerable to earthquake events [2–5]; since then the antiseismic design of underground structures has become a subject of intense research all over the world [6–8].

Seismic design of underground structures has been studied via two main approaches [9]: nonlinear dynamic numerical modelling by finite element method or finite difference method [10] and simplified seismic design based on quasistatic method. The nonlinear dynamic numerical analysis is complex and not practical for engineers, due to the computation inefficiency as well as the complexity of discretization, wave-absorbing boundaries, and wave-motion input. Meanwhile, simplified seismic design methods are highly popular in preliminary design for their efficiency

and convenience, including free-field deformation method [11], simplified frame analysis method [12, 13], response displacement method [14, 15], and pushover analysis method [16]. In these methods, the response displacement method has been adopted by the seismic design codes [17–19] for underground structures in China more than any other quasistatic methods because of its clear physical concept and simple calculation. The response displacement method can evaluate the force applied to the underground structures derived from soil deformation; simultaneously, the complex mechanical properties of soil can be avoided during the calculation process. The schematic diagram of response displacement method is shown in Figure 1; underground structure is subject to the inertial force and the shear stress around the structure as well as the spring force. Subgrade springs include horizontal normal springs, horizontal shear springs, vertical normal springs, and vertical shear springs; the spring force can be obtained by applying the soil deformation to the end of the spring and the stiffness of spring equal to the subgrade reaction coefficient times the stressed area.

The most critical parameter regarding the analysis through response displacement method is the subgrade reaction coefficient of soil, which has a significant effect on the precision of calculating results; subgrade reaction coefficient denotes the ratio of pressure to displacement at the same point. Carrying out test (i.e., in-site and laboratory tests) is the most reliable way to acquire subgrade reaction coefficient of soil. In-site tests including plate loading test (PLT) and pressure meter test (PMT) are widely applied to obtain subgrade reaction coefficient. Furthermore, alternative laboratory testing methods include consolidation test and triaxial test [20]. PLT was originally proposed by Terzaghi [21]. Burhan and Ayhan [22] evaluated the relationship between subgrade reaction coefficient and displacement magnitude by 43 full-scale plate loading tests and indicated that coefficient decreased with an increase in displacement of soil. Lin et al. [23] employed plate loading test with different plate diameters to evaluate subgrade reaction coefficient of gravelly cobble deposit in Taichung Basin, Taiwan. Choi et al. [24] compared subgrade reaction coefficients of permeable block pavement site and aggregate base site by plate loading test and pointed out that permeable block had a higher structural ability. Firuzi et al. [25] proposed correlation of corrected standard penetration test number with subgrade reaction coefficient obtained by pressure meter test. Yu and Tang [26] discovered that loess subgrade reaction coefficients acquired by pressure meter test were 0.5 to 2 times of results acquired by plate loading test. Pan et al. [27] proposed revised method in terms of height and diameter to measure subgrade reaction coefficient in soft soil area through consolidation test. Yin et al. [28] implemented triaxial test to evaluate subgrade reaction coefficient of granite residual soil and concluded that the expression between the stress and strain had the best linear dependence when the ratio of lateral stress increment to axial stress increment equaled 0.1. Herein, a brief review of the features and drawbacks of these kinds of testing techniques is described as follows:

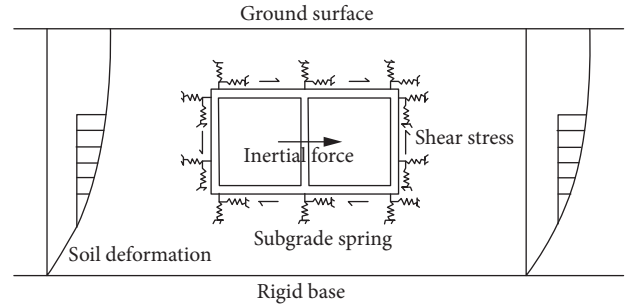

Figure 1: Schematic diagram of response displacement method.

(1) Soil deformation and strength properties can be assessed in terms of soil load-displacement relationship which is obtained by PLT. Testing well generally needs to be dug to the specified depth before applying load in PLT, so it is not fit for the deep-buried conditions. Additionally, PLT is usually limited to the drawbacks, viz., waste of time, high cost, loading direction, and size effect of plate.

(2) The probe is set in the test hole with specified depth; soil pressure-volume relationship then can be acquired by PMT. High quality is required for drilling and it is not suitable for gravels and rocks. Furthermore, horizontal subgrade reaction coefficient determined via PMT is on the basis of the axially symmetric hypothesis, which cannot reflect the sophisticated influence of anisotropic soil.

(3) Subgrade reaction coefficient can also be evaluated by the consolidation test and triaxial test. However, the size and the confining pressure condition of soil samples are not consistent with the in-site soil; thus, the reliability of testing results is quite limited.

The analyses above expound problems of existing testing methods for subgrade reaction coefficient, such as questionable accuracy of measured results, limited environments for application, high cost, and unrealistic assumption of soil condition. In order to overcome drawbacks of existing laboratory test methods and obtain subgrade reaction coefficient suitable for antiseismic design of underground structures, this study makes an attempt to apply novel laboratory testing methods considering realistic seismic response of soil. A shaking table test and a new test technique, namely, quasistatic test, have been proposed to evaluate horizontal subgrade reaction coefficient. Meanwhile, a novel quasistatic pushover device is developed according to the requirements of quasistatic testing method. The most unfavorable deformation mode of soil during earthquake event [29] can be achieved by the new testing system. These tentative tests are performed for solving practical engineering problems with more options.

2. Shaking Table Test

Antiseismic design of underground structures is mainly dealing with shear wave propagating vertically upward from bed rock. This kind of wave will lead to horizontal shear

deformation of soil strata; therefore, horizontal subgrade reaction coefficient is the main research goal in this section, including horizontal shear subgrade reaction coefficient and horizontal normal subgrade reaction coefficient.

2.1. Shaking Table System. The test was conducted in the Key Laboratory of Earthquake Engineering and Engineering Vibration in Institute of Engineering Mechanics of China Earthquake Administration. The dimension of the shaking table is 5 m × 5 m. The shaking table is capable of 300 kN payload. The maximum acceleration of the shaking table is ±1 g, where g represents acceleration due to gravity. Meanwhile, the maximum horizontal displacement of the shaking table is ±80 mm.

2.2. Shear Stack. The objective of the shaking table test is to investigate the unfavorable deformation and horizontal subgrade reaction coefficient of the sandy free-field; thus, a soil container is needed. The shear stack employed in the test was a large-sized multifunctional laminar container with a dimension of 3.5 m (long) × 2.4 m (wide) × 1.7 m (high), which was developed by our own research group. The stack can move in two directions; its steel rings can move freely along the direction of vibration due to little steel balls in the ring interlayers, while the response perpendicular to the direction of vibration is limited by a system composed of bearings and rigid steel frame. The base surface of the stack is rough enough to deliver complementary shear stress, and the side walls can absorb reflected wave through flexible rubber pad. Sun et al. [30] demonstrated that the stack can effectively eliminate the boundary effect by performing finite element analysis and a series of shaking table tests.

As shown in Figure 2, the shear stack was installed with its long side corresponding to the shaking direction of the shaking table during the dynamic test.

2.3. Testing Soil. Combining the Unified Soil Classification System with the grain size distribution curve of testing soil (as shown in Figure 3), the soil used in the shaking table test can be classified as poor-graded sand with uniformity coefficient (C_u) equal to 2.8 and coefficient of curvature (C_c) equal to 0.9. Furthermore, specific gravity of soil grain (G_s) is 2.66, the average moisture content (ω) is 6%, the natural density (ρ) equals 1.6 g/cm^3, and the maximum and minimum dry sand density ($\rho_{d\max}$ and $\rho_{d\min}$) equal 1.88 and 1.38 g/cm^3, respectively (i.e., the relative density (D_r) is 51%). Last but not least, sand cohesion (c) of 4 kPa and internal friction angle (φ) of 35° are obtained by direct shear test.

The maximum height of the sandy field in the test was set to 1.2 m. Before the test, the testing soil was filled into the stack layer by layer (the height of each layer reached 0.2 m, and the targeted marks were placed on the inner side of the stack). Each sand layer was tamped using a special hammer. The hammer was lifted and placed against each layer surface repeatedly till the ultimate thickness was reached. Simultaneously, the soil samples were taken out for test to ensure that the sand density of each layer was consistent.

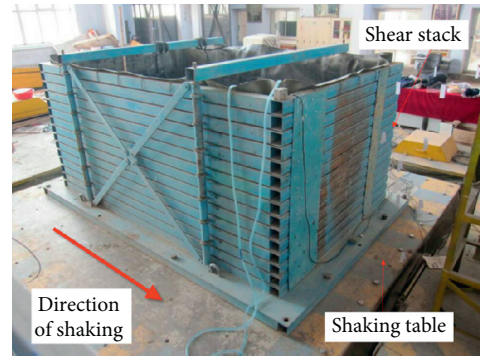

Figure 2: The shear stack installed on the shaking table.

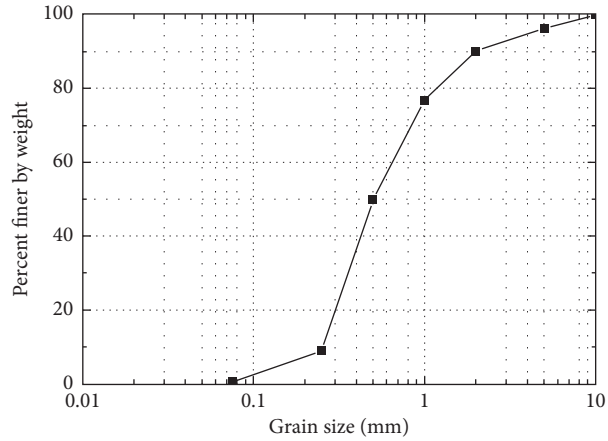

Figure 3: Grain size distribution curve.

2.4. Experimental Set-Up and Excitation. Two parameters (i.e., acceleration and soil stress) were considered in the present test, so two kinds of transducers were applied to the test so as to obtain the objective data during the shaking process. Four accelerometers (A1–A4) were embedded inside of the sand deposit at similar coordinate in the horizon plane, and the vertical interval between two accelerometers was 0.3 m. Meanwhile, three earth pressure cells (P1–P3) were embedded beside the positions of A1–A3 separately; the stress surfaces of the earth pressure cells were perpendicular to the direction of vibration to measure horizontal normal stress of soil. Figure 4 portrays the arrangement of sensors adopted in shaking table test.

Considering the model dimension, the scaled acceleration record of El-Centro wave was chosen as the input motion. The input acceleration time history and the corresponding Fourier spectra contents information are shown in Figure 5. Varying peak acceleration amplitude was mainly considered in the experimental cases. It can be drawn that the frequencies of the shaking wave were mainly in a range of 3~7 Hz. Before applying the excitation to the test, the amplitude of the signal in time domain was adjusted so as to match three levels of earthquake intensity; the input peak acceleration values were set to 0.1 g, 0.2 g, and 0.4 g respectively.

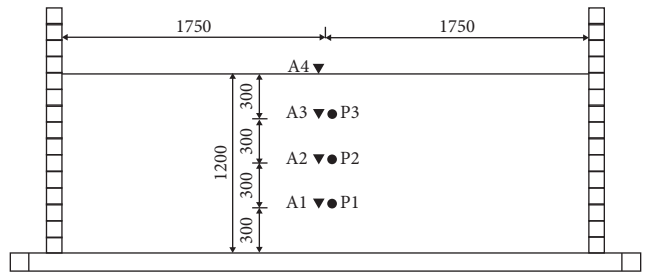

Figure 4: Arrangement of sensors embedded in observation section for shaking table test (units: mm) (A: accelerometer; P: earth pressure cell).

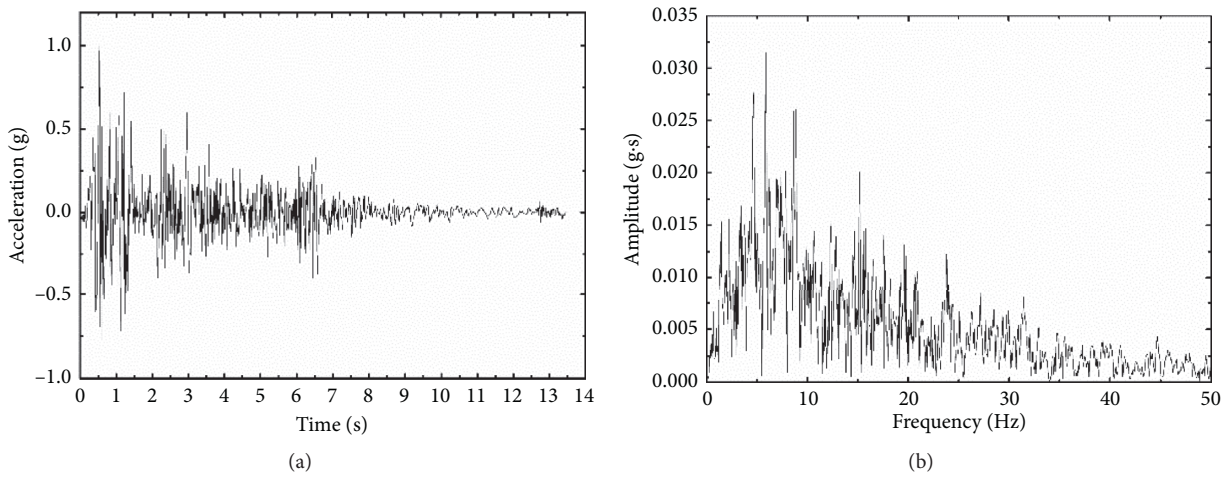

Figure 5: Input El-Centro wave. (a) Time history of acceleration. (b) Fourier spectrum.

2.5. Result and Analysis. The shaking table test helped identify unfavorable deformation and the corresponding subgrade reaction mechanism of sandy free-field, which are not included in the current testing methods for analysis of subgrade reaction coefficient. During dynamical test, acceleration and stress of soil with a different level of input peak acceleration (i.e., 0.1 g, 0.2 g, and 0.4 g) were obtained. Analyses and discussions of the testing results mainly focus on holistic hysteresis curve and equivalent subgrade reaction coefficient derived from typical hysteresis loop.

It is necessary to provide a comprehensive introduction of soil shear stress calculation method for better understanding the follow-up analytical work. The recorded acceleration time histories at diverse depths along the soil deposit can be used to back-calculate the values of shear stress with integral transformation. To date, the calculation method has been widely adopted [31]. Supposing that a 1D shear wave propagates vertically, then the soil deposit can be regarded as an idealized shear beam model. The assumption for soil is reasonable in shear stack where shear deformation is predominant. Based on the principles mentioned above, the approximated estimation values of shear stress can be acquired at any soil depth; schematic diagram of calculation is presented in Figure 6:

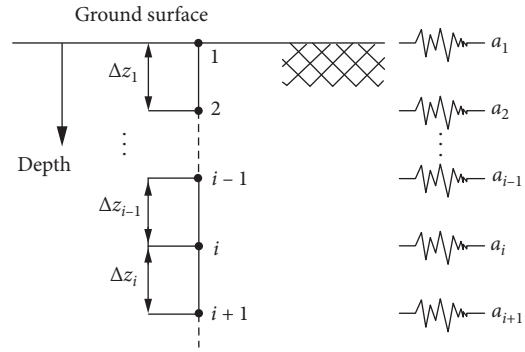

Figure 6: Sketch for computing shear stress in the model soil.

$$T(z,t) = \int_0^z \rho a(\xi,t)\mathrm{d}\xi. \tag{1}$$

By means of linear interpolation between adjacent transducers, the discrete data points can be used to calculate shear stress (T) at any time and any soil depth field according to the following formula derived from formula (1):

$$T(z_i,t) = T(z_{i-1},t) + \rho\frac{a(z_{i-1},t) + a(z_i,t)}{2}\Delta z_{i-1}, \tag{2}$$

where Δz_i is the vertical interval between depths z_i and z_{i+1} as shown in Figure 6; $T(z_i, t)$ is the shear stress of the soil depth z_i at the time t; $T(z_{i-1}, t)$ is the shear stress of the soil depth z_{i-1} at the time t; $a(z_i, t)$ is the horizon acceleration of the soil depth z_i at the time t; $a(z_{i-1}, t)$ is the horizon acceleration of the soil depth z_{i-1} at the time t; and ρ is the mass density of the soil. The shear stress obtained by this way has second-order accuracy.

2.5.1. Holistic Hysteresis Curve. Horizontal shear stress of soil during the shaking process can be investigated by integral transformation program which is previously proposed. Horizontal displacement is acquired by quadratic integration of acceleration, while the horizontal normal stress can be directly measured. A Butterworth filter with a passband from 0.5 Hz to 10 Hz is employed.

The dynamic responses of the sandy free-field can be estimated in terms of hysteresis curves. Based on the calculation procedures mentioned above, the hysteresis curves of the calculated horizontal shear stress with respect to the horizontal displacement (i.e., T-D) and the hysteresis curves of the measured horizon normal stress with respect to the horizontal displacement (i.e., P-D) of observation points along the center line in the dynamic test are illustrated in Figure 7. On the whole, the horizontal displacements, horizontal shear stresses, and horizontal normal stresses of soil increase gradually with excitation amplitude; meanwhile, the horizontal displacements of soil decrease gradually with the increasing depth (i.e., the maximum horizontal displacements at depth of 0.3 m, 0.6 m, and 0.9 m under 0.4 g excitation are 3.508 mm, 2.447 mm, and 1.544 mm, resp.) and the shape of the soil deformation is in an invert triangle order [16]. It is worth noting that the shear stresses and the normal stresses of the soil change synchronously under seismic excitation, and these two kinds of holistic hysteresis curves are similar in shape.

Figure 7 plots the hysteretic behavior of soil under different input amplitude; the holistic hysteresis curves under 0.1 g excitation describe several conspicuous loops with varying inclination; the soil exhibits apparent nonlinearity during the shaking process. As the input amplitude increases, the holistic hysteresis curves become more and more rounded; particularly those under 0.4 g excitation, the soil stiffness degrades distinctly. On the other hand, the damping increases with input amplitude; the increasing damping force can lead to the energy dissipation of soil field by plastic yielding, which can be reflected by the significantly increasing hysteresis area. The degrees of stiffness attenuation and energy dissipation in sandy free-field depend on the amplitude of excitation.

2.5.2. Typical Hysteresis Loop. The maximum deformation of soil field under earthquake motion is employed in simplified seismic design method. Further analyses of soil subgrade reaction coefficient are carried out by representing the outmost hysteresis loops extracted from the holistic hysteresis curves. Figure 8 depicts the typical hysteresis loops. The evaluations of the difference between maximum and minimum displacements and the difference between corresponding shear stresses and normal stresses developed in the hysteresis loops are adopted to calculate the equivalent subgrade reaction coefficient of soil. The equivalent subgrade reaction coefficient can be given by

$$K_S = \frac{T_a - T_b}{D_{\max} - D_{\min}}, \tag{3}$$

$$K_N = \frac{P_a - P_b}{D_{\max} - D_{\min}}, \tag{4}$$

$$R_K = \frac{K_N}{K_S}, \tag{5}$$

where K_S is the equivalent shear subgrade reaction coefficient, K_N is the equivalent normal subgrade reaction coefficient, $D_{\max}$ and $D_{\min}$ are the maximum and minimum displacements in the typical hysteresis loop, T_a and T_b are the shear stresses corresponding to $D_{\max}$ and $D_{\min}$, P_a and P_b are the shear stresses corresponding to $D_{\max}$ and $D_{\min}$, and R_K is the ratio of K_N to K_S.

The result is summarized in Table 1, which indicates that the horizontal equivalent shear subgrade reaction coefficient (K_S) and the equivalent normal subgrade reaction coefficient (K_N) decrease with shaking intensity (i.e., K_S at depth of 0.9 m under 0.1 g, 0.2 g, and 0.4 g excitation are 7.922 MN/m^3, 4.532 MN/m^3, and 2.298 MN/m^3; K_N are 19.568 MN/m^3, 14.366 MN/m^3, and 9.234 MN/m^3, respectively). Furthermore, K_S and K_N increase with soil depth (i.e., K_S at depth of 0.3 m, 0.6 m, and 0.9 m under 0.4 g excitation are 0.224 MN/m^3, 0.933 MN/m^3, and 2.298 MN/m^3; K_N are 1.441 MN/m^3, 4.826 MN/m^3, and 9.234 MN/m^3, separately). The code for geotechnical investigations of urban rail transit in China has summarized the empirical values of subgrade reaction coefficient [32] (as listed in Table 2). As a result of comparative analysis, the values of K_N (1.441 MN/m^3~19.568 MN/m^3) are within a reasonable scope.

The two typical kinds of outmost hysteresis loops at the same observation point are similar in shape. As calculated via (5), there seems to be a proportional relationship between K_S and K_N, which can be concluded from Table 1. The comprehensive calculation values show that R_K is not a constant value, which ranges from 2.47 to 6.43 with the fluctuation of shaking intensity and soil depth.

It is evident that R_K degradation depends on the input peak amplitude. This phenomenon can be well explained by the fact that soil is composed of many scattered tiny particles; compressive strength of soil is much larger than shear strength. In general, soil failure results from shear failure, so it is not difficult to understand that the strength of soil is defined in terms of shear strength. As input amplitude increases, the resistances of soil to shear stress and normal stress gradually decrease until the soil turns into the plastic stage. They are not to scale (i.e., the decline proportion of shear stress is even more) since the former is much more sensitive to shaking intensity.

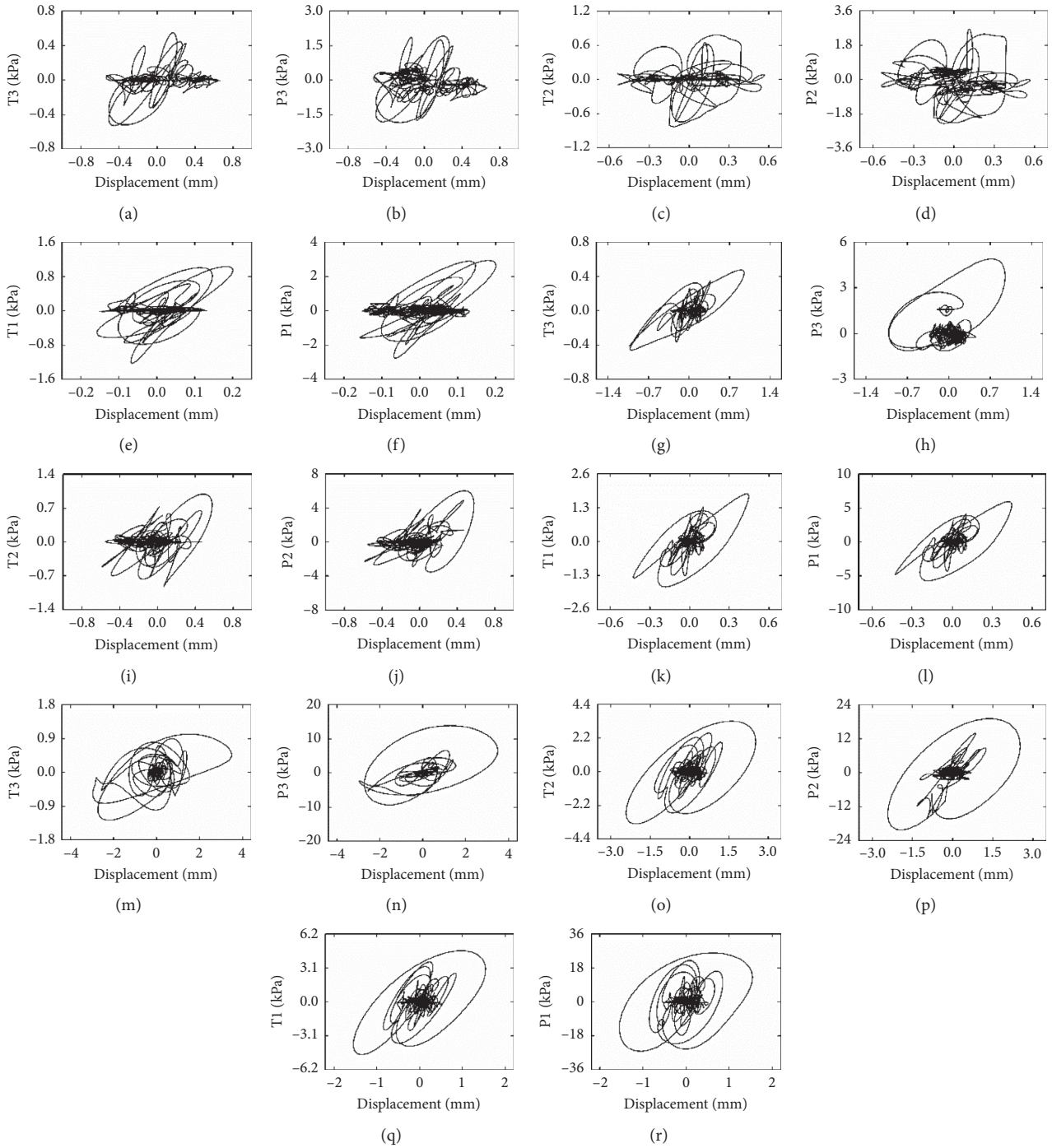

Figure 7: Hysteresis curves of horizontal normal stress and shear stress versus displacement: (a) (b) T3 and P3 under 0.1 g excitation. (c, d) T2 and P2 under 0.1 g excitation. (e, f) T1 and P1 under 0.1 g excitation. (g, h) T3 and P3 under 0.2 g excitation. (i, j) T2 and P2 under 0.2 g excitation. (k, l) T1 and P1 under 0.2 g excitation. (m, n) T3 and P3 under 0.4 g excitation. (o, p) T2 and P2 under 0.4 g excitation. (q, r) T1 and P1 under 0.4 g excitation.

On the other hand, Table 1 also indicates that the R_K values decrease gradually as soil depth increases. This discovery is consistent with the simplified frame analysis method [13] which suggests simulating the influence of soil on underground structures during earthquake by applying a concentrated force on roof of underground structures for deep burial conditions (i.e., shear stress plays a leading role in the forces of causing structural deformation) or applying invert triangle shaped uniform force on side wall of underground structures for shallow burial conditions (i.e.,

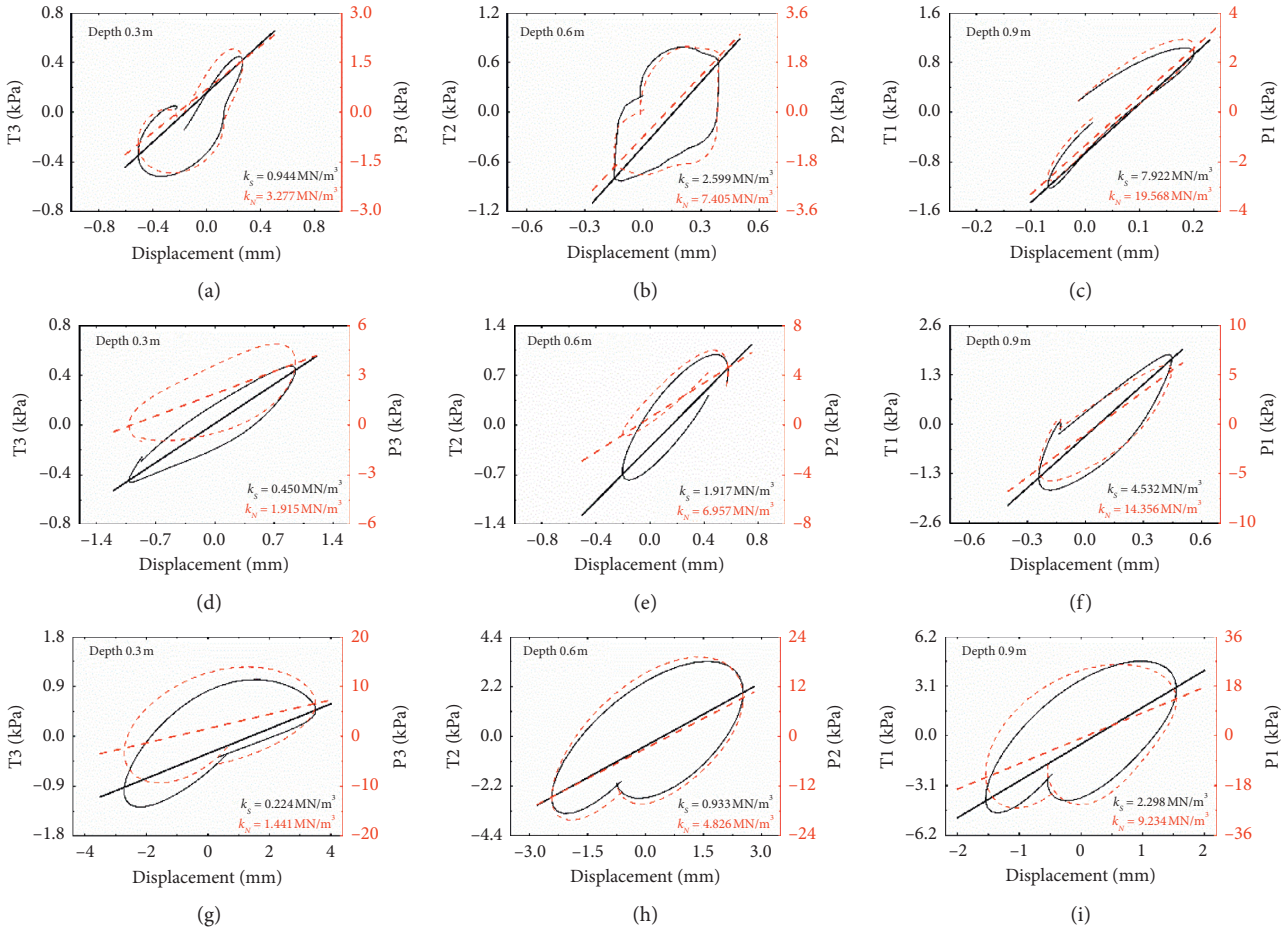

Figure 8: Presentative hysteretic loops of soil: (a) T3 and P3 under 0.1 g excitation. (b) T2 and P2 under 0.1 g excitation. (c) T1 and P1 under 0.1 g excitation. (d) T3 and P3 under 0.2 g excitation. (e) T2 and P2 under 0.2 g excitation. (f) T1 and P1 under 0.2 g excitation. (g) T3 and P3 under 0.4 g excitation. (h) T2 and P2 under 0.4 g excitation. (i) T1 and P1 under 0.4 g excitation.

Table 1: The horizontal equivalent subgrade reaction coefficients and ratios of soil.

Peak amplitude (g)	Depth (m)	K_S (MN/m^3)	K_N (MN/m^3)	R_K
0.1	0.3	0.994	3.277	3.30
	0.6	2.599	7.405	2.85
	0.9	7.922	19.568	2.47
0.2	0.3	0.450	1.915	4.26
	0.6	1.917	6.957	3.63
	0.9	4.532	14.366	3.17
0.4	0.3	0.224	1.441	6.43
	0.6	0.933	4.826	5.17
	0.9	2.298	9.234	4.02

horizontal normal stress dominates structural deformation) (as shown in Figure 9), demonstrating that the change law of R_K values along depth is reliable.

3. A Novel Quasistatic Device

Owing to the complexity of soil properties, high cost, and transient response to dynamical excitation, thus shaking table test is limited to evaluate variation tendency of horizontal subgrade reaction coefficient qualitatively. Quasistatic test is known as a preferable testing method with better stability for quantitative analysis of stress mechanism in structural domain [33, 34], which provides a new approach for evaluation of horizontal subgrade reaction coefficient. A difficulty arises in quasistatic testing method which is the gap in quasistatic soil container. Existing soil containers are mainly appropriate for dynamic tests. Hence, a novel soil container and corresponding loading system designed for quasistatic test are developed in consideration of soil deformation mode, buried depth, boundary condition, dimension of soil sample, and visualization.

Table 2: Empirical values of the subgrade reaction coefficient.

Soil category	Status	Subgrade reaction coefficient (MN/m^3)	
		Horizontal normal	Vertical normal
Sandy soil	Loose	3~15	5~15
	Slightly less dense	10~30	12~30
	Medium dense	20~45	20~40
	Dense	25~60	25~65

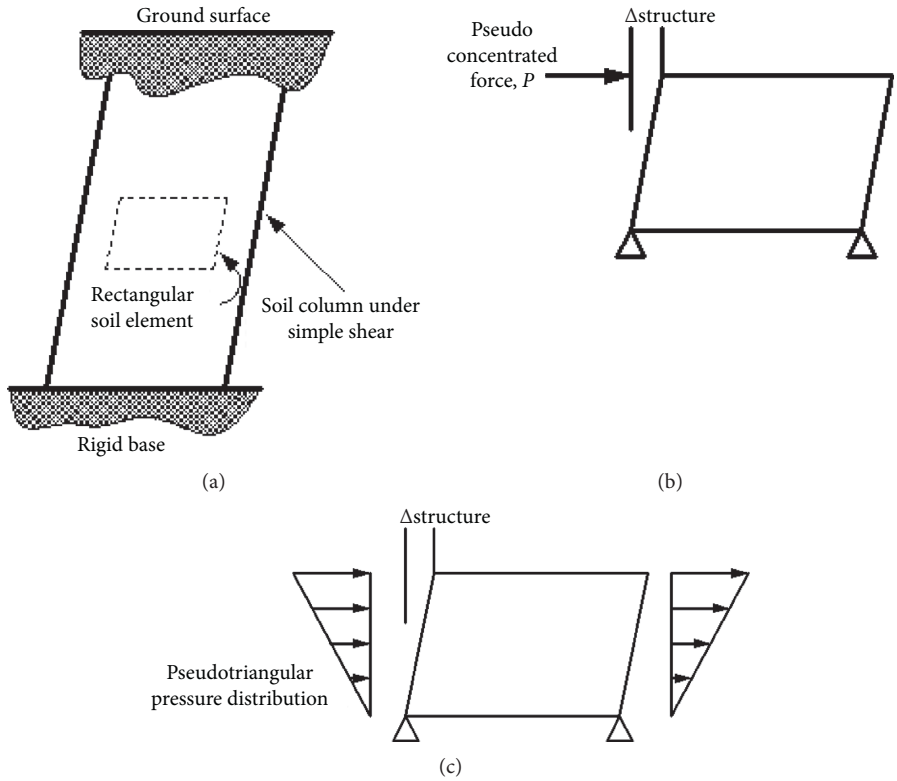

FIGURE 9: Simplified frame analysis mode (after Wang [13]). (a) Shear distortion of free-field soil medium. (b) Pseudoconcentrated force for deep tunnels (shear stress on the roof). (c) Pseudotriangular pressure distribution for shallow tunnels (normal stress on side wall).

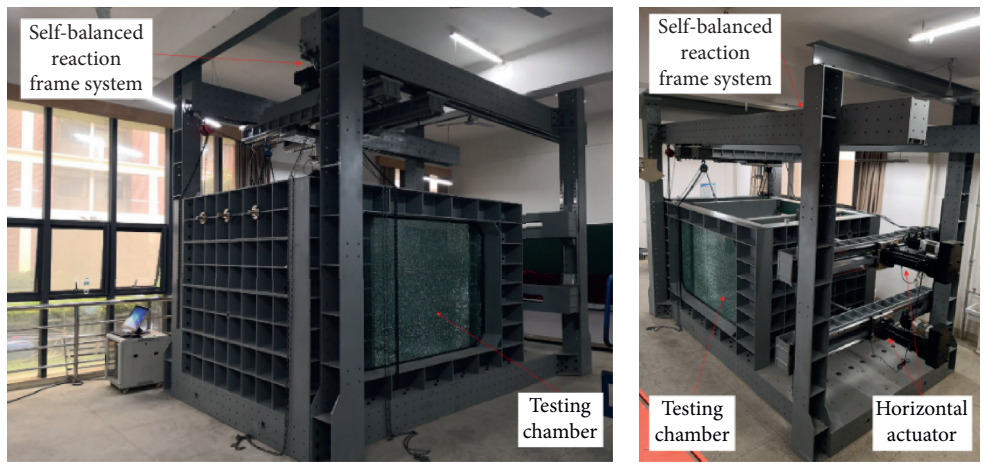

FIGURE 10: The quasistatic testing device assembled on the ground. (a) View from passive side. (b) View from push side.

3.1. Construction of the New Testing Device. The innovative multifunctional testing system has been constructed for quasistatic test as depicted in Figure 10. It consists of a testing chamber with two interior adjustable slide plates and a self-balanced reaction frame system.

In regard to the exterior frame of testing chamber, two parallel walls inlaid with tempered glass are set along the loading direction; the other two end walls composed of four fabricated grid plates are set perpendicular to the loading direction. There are two slide plates located parallel to end grid plates, which can rotate around the bottom, thus, satisfying the needs of deformation mode and adjustable inner space. Since these two slide plates have been installed, interior net dimension of testing chamber is 2 m × 2 m × 2 m in this test. The pushover slide plate is connected to two parallel horizontal actuators via spherical hinges and slide rails. Opposite slide plate is connected to end wall by three springs with adjustable stiffness. The stiffness is set to 14 N/

mm in this test, the horizontal displacements of the bottom of slide plates are restricted by three convex blocks, and the schematic diagram of testing chamber is illustrated in Figure 11. The circular drainage holes are set at the bottom of the testing chamber as a consideration of soil drainage, which can be covered by permeable stones during the test (as presented in Figure 12).

The self-balanced reaction frame system is composed of a steel raft base with the dimension of 5 m × 2.5 m × 0.3 m, four groove profile columns with the dimension of 0.25 m × 0.25 m × 3.78 m, two box profile girders with the dimension of 0.4 m × 0.25 m × 5.5 m, two box profile secondary beams with the dimension of 0.35 m × 0.25 m × 3 m, two H profile joining beams with the dimension of 0.35 m × 0.25 m × 3 m, and two groove profile horizontal loading beams with the dimension of 0.25 m × 0.25 m × 3 m, respectively. The actuator mounted on the secondary beam can offer vertical load and two actuators installed on horizontal loading beam can provide horizontal load; each of the actuators is capable of 200 kN payload.

3.2. Features of the New Testing Device. Original features of this novel testing device are as follows:

(1) In general, the most unfavorable deformation mode of soil under seismic motion is akin to an invert triangle. Invert triangle shaped deformation of soil can be realized through horizontal pushover system. Consequently, increasing earthquake intensity can be simulated by controlling the rotation angle of the pushover slide plate.

(2) Buried depth is the key parameter affecting subgrade reaction coefficient. In practical terms, an underground structure generally has a certain buried depth. The vertical actuator can provide additional stress to represent upper covered soil.

(3) The interaction of soil can be considered as springs in parallel with dashpots in dynamical analysis; however, it can be purely simplified as springs in static analysis. The springs with adjustable stiffness employed in the device can simulate the effect of the infinite domain soil on the selected soil in the container during test.

(4) Affected by the size of soil sample, basic soil mechanics law that the additional stresses decrease with distance is usually unachievable in previous laboratory testing methods. Herein, two slide plates in the testing chamber can adjust the volume of testing chamber to meet the dimension demand.

(5) Different from the transient response in shaking table test, quasistatic method refers to decomposing the continuous seismic motion into a series of small steps and completing the whole process step by step in sequence. Visualization of soil deformation process at each loading step is also an innovative highlight.

(6) Taking advantage of its high quality, easy transformation, environmentally friendly nature, and multifunction, this novel device represents the new application of the mature fabricated technology that satisfies the requirement of sustainable development.

4. Quasistatic Testing Verification

Based on the novel device, the proposed quasistatic method in this research can be implemented. Rapid-changed soil deformation under dynamic excitation can be broken up into several static stages in terms of specified deformation mode; meanwhile, the stress state of soil can be obtained by the means.

4.1. Testing Soil. The maximum height of the sandy field in quasistatic test was 1.8 m; the soil material and method of filling soil used in the quasistatic test were the same as shaking table test, for the sake of getting a quantitative value corresponding to the same soil properties.

4.2. Experimental Set-Up. For the purpose of identifying the horizontal subgrade reaction coefficients by quasistatic test, three types of transducers were required. A shape acceleration array (SAA) [35, 36] was mounted in the middle of the testing chamber to monitor horizontal soil displacement; six measuring points were evenly distributed along SAA with an interval of 30 cm. Fifteen earth pressure cells T1~T15 were embedded in soil deposits corresponding to different depths of SAA measuring points, respectively; the earth pressure cell matrix of five rows and three columns came into being. According to the numerical calculation in the preliminary stage, the range of the earth pressure cells was 0–400 kPa, and the sampling frequency of the earth pressure cells was 1 Hz due to the low frequency of the test. Moreover, two linear variable differential transformers (LVDT D1 and D2) were installed to measure the horizontal displacement of the pushover slide plate as high as soil surface; arrangement of sensors is presented in Figure 13.

4.3. Loading Program. The loading program of quasistatic test was quite different from that of shaking table test. The two slide plates remained vertical at initial stage. To implement invert triangle shaped soil deformation mode caused by earthquake, the pushover slide plate was pushed by horizontal actuators. The whole loading program was controlled by the rotation angle of the pushover slide plate. The specified rotation angles are listed in Table 3.

$$\alpha = \frac{D}{H}, \tag{6}$$

where α denotes the rotation angle of pushover plate, D denotes the measured horizontal displacement of pushover plate at the height of soil surface, and H denotes the height of soil.

4.4. Experimental Results and Analysis. Observation data for analysis of subgrade reaction coefficients in sandy site mainly contains the horizontal displacement and the horizontal normal stress of soil.

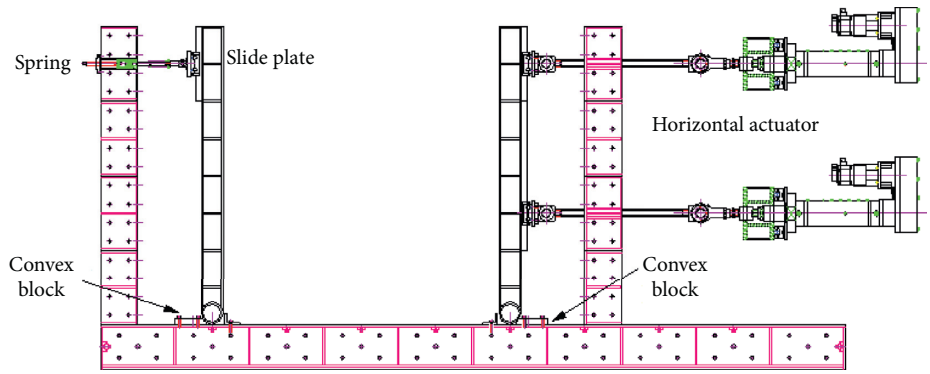

Figure 11: Schematic diagram of testing chamber.

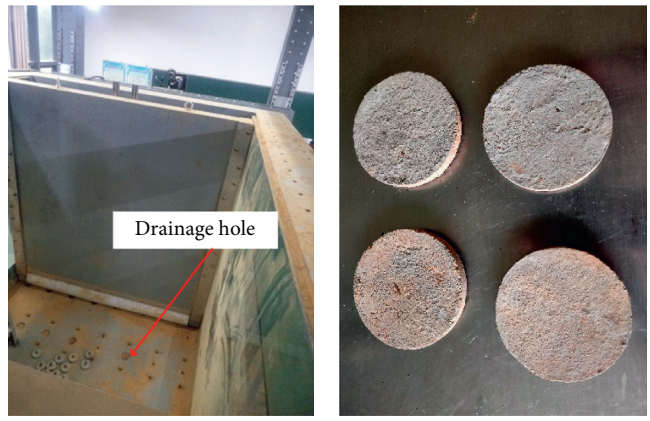

(a) (b)

Figure 12: Drainage system. (a) Drainage holes. (b) Permeable stone.

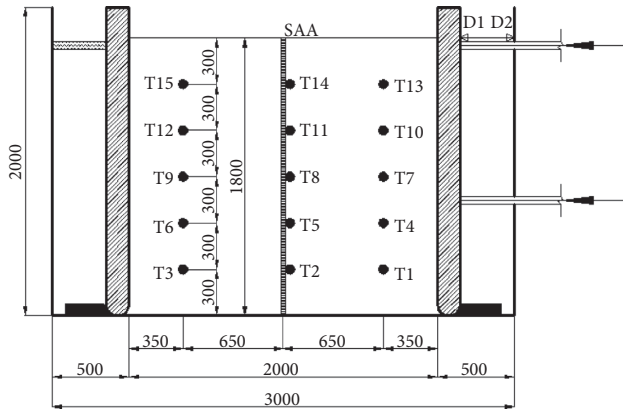

Figure 13: Arrangement of sensors embedded in observation section for quasistatic test (units: mm) (D: LVDT; T: earth pressure cell; SAA: shape acceleration array).

Table 3: The selected rotation angle for analysis.

State	Rotation angle	State	Rotation angle
1	1/1800	8	1/100
2	1/900	9	1/75
3	1/600	10	1/60
4	1/400	11	1/50
5	1/300	12	1/40
6	1/200	13	1/30
7	1/150		

4.4.1. Soil Displacements. The horizontal displacements of soil supervised by SAA are calculated and reported in Figure 14. Soil displacements at different depths increase as rotation angle of pushover plate increases. An invert triangle soil deformation trend along buried depth is revealed. The soil deformation mode shows a high consistency with the most disadvantageous deformation mode observed in free-field shaking table test. Since the voids are compacted in the soil close to the pushover slide plate, the deformation attenuation in transit then occurs. It is clearly reflected by the maximum displacement of soil surface which is approximately equal to one-third of that measured in the pushover slide plate at the same height.

4.4.2. Horizontal Stress. Figure 15 plots the measured horizontal stresses at different observation positions; horizontal stresses increase with rotation angle of pushover plate; in other words, the additional stresses increase with soil displacement. Another conclusion that the additional stresses decrease with the distance from the measuring point to the pushover plate at the same buried depth can be drawn from Figure 15. The soil stress

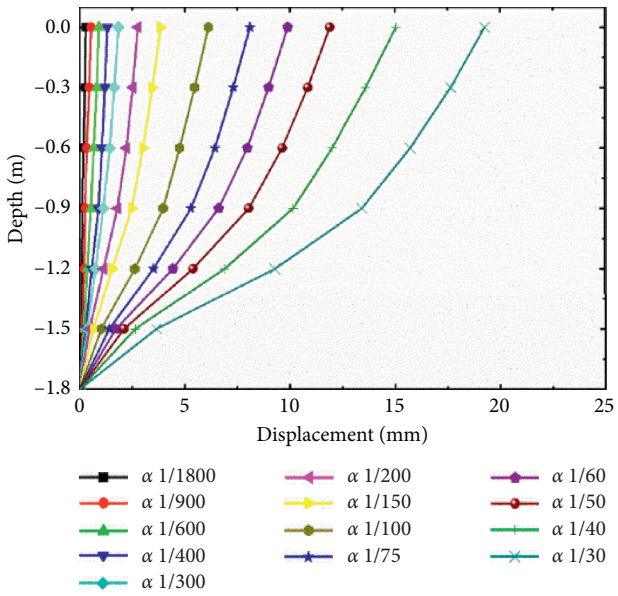

Figure 14: Horizontal displacement of soil.

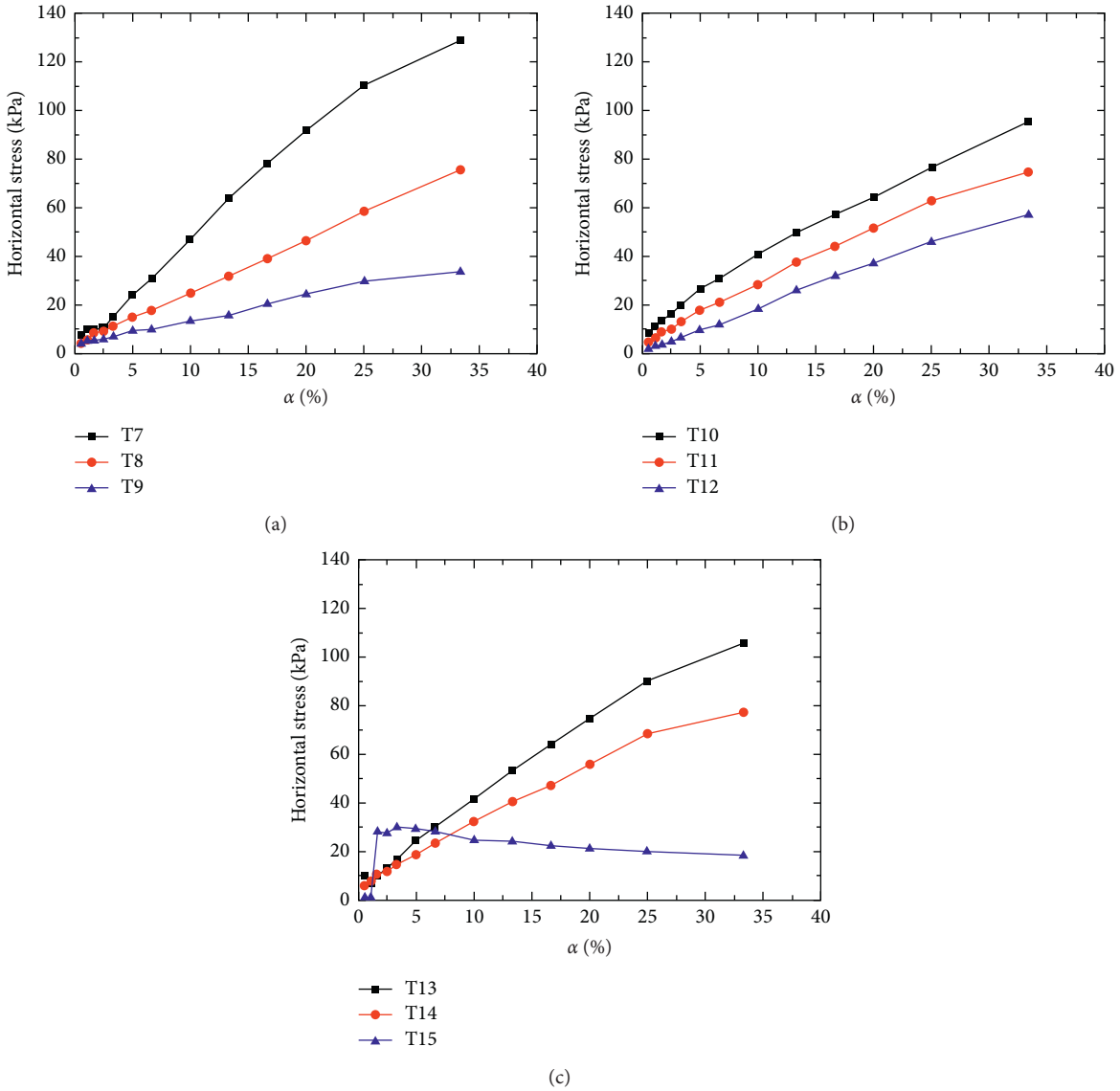

Figure 15: Horizontal stress of soil. (a) Depth of 0.9 m. (b) Depth of 0.6 m. (c) Depth of 0.3 m.

condition distribution trends are agreed with those in load plate test [22] (the anomaly of T15 earth pressure cell may owe to breakdown).

4.4.3. Subgrade Reaction Coefficient. The horizontal normal subgrade reaction coefficients can be evaluated on the basis of the horizontal displacements and stresses of soil. The relationship between the horizontal normal subgrade reaction coefficient and the rotation angle of pushover plate is summarized in Figure 16. With the small rotation angle of 1/1800, the measured maximum horizontal normal subgrade reaction coefficients range from 20 MN/m^3 to 37 MN/m^3 at the buried depth from 0.3 m to 1.5 m, respectively. The horizontal normal subgrade reaction coefficients nonlinearly decrease with the rotation angle. With the large rotation angle of 1/30, the minimum horizontal normal subgrade reaction coefficients range from 4.4 MN/m^3 to 7.4 MN/m^3 at the buried depth from 0.3 m to 1.5 m, respectively; the horizontal subgrade reaction coefficients decrease with the horizontal displacement of soil increasing. As the status of soil gradually changes from elasticity stage into plasticity stage during the loading process, horizontal normal subgrade reaction coefficients drop sharply. And then, the recession develops slowly with the rotation angle since subgrade reaction coefficient tends to be stable after the soil becomes completely plastic. It is also obvious from Figure 16 that the horizontal normal subgrade reaction coefficients increase with depth at the same rotation angle; these rules are in agreement with the results from dynamic test.

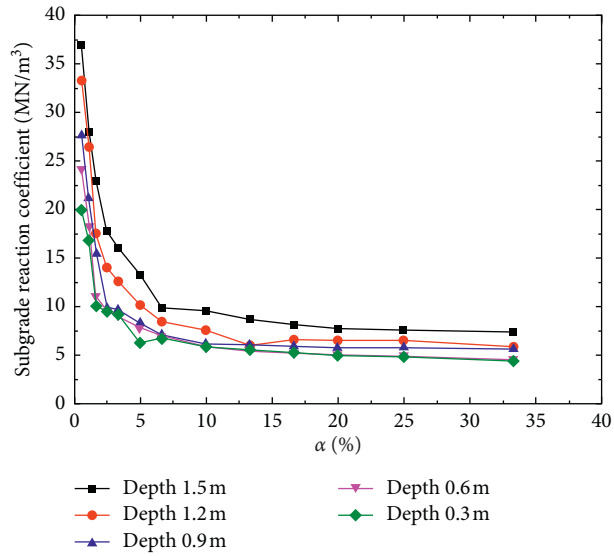

Figure 16: Horizontal normal subgrade reaction coefficients versus rotation angle.

5. Summary and Conclusions

Concentrated foundation spring derived in terms of the subgrade reaction coefficient is usually implemented into simplified antiseismic design of underground structures preliminarily. Laboratory test is an effective method for calculating the subgrade reaction coefficient. However, due to the limitations in existing laboratory tests, it is difficult to investigate the credible subgrade reaction coefficient for further antiseismic study. In this investigation, a shaking table test of sandy free-field was presented for estimating the seismic behavior of soil and firstly trying to calculate the horizontal equivalent subgrade reaction coefficient. Based on the testing work, some meaningful results can be summarized:

(1) The dynamic hysteretic curves of horizontal shear stress and normal stress with respect to soil displacement obtained in the shaking table test are similar in shape. Maximum horizontal displacements of soil decline gradually with buried depth, which also verify that the most unfavorable deformation mode of soil under seismic excitation is in a shape of an invert triangle.

(2) Equivalent shear subgrade reaction coefficient and equivalent normal subgrade reaction coefficient can be calculated from the outmost hysteresis loops extracted from the holistic hysteresis curves. Comparing with the empirical values of subgrade reaction coefficient in code for geotechnical investigations of urban rail transit in China, the experimental values of horizontal equivalent normal subgrade reaction coefficient (range from 1.441 MN/m^3 to 19.568 MN/m^3) are within a reasonable scope.

(3) The ratio of equivalent normal subgrade reaction coefficient to equivalent shear subgrade reaction coefficient varies from 2.47 to 6.43; it is apparently not a constant value; the ratio increases with increasing shaking intensity and decreases with growing buried depth.

Considering the disadvantages of high cost and transient response of shaking table test, the first attempt at application of a quasistatic pushover method was then reported. A novel multifunctional device for quasistatic test was constructed to implement the testing schedule. Within the analytical testing results, the following can be concluded:

(1) The novel multifunctional device can meet the requirements of quasistatic testing method, i.e., invert triangle soil deformation mode, low cost, varying buried depth, geometric dimension, boundary condition, and easy transformation. This innovative device also represents the new application of the mature fabricated technology which meets the demand of sustainable development.

(2) The verification quasistatic testing results indicate that subgrade reaction coefficients decrease with increasing soil displacement and increase with increasing buried depth, which is consistent with the laws found in the shaking table test. The reliability of the experimental subgrade reaction coefficient is confirmed by comparing with Chinese standard for geotechnical investigations of urban rail transit.

It should be noted that the subgrade reaction coefficient depends on the soil type, soil properties (e.g., density or relative density, moisture content, internal friction angle, and the degree of consolidation), and loading directions. The results and conclusions presented in the literature are available for the test condition (i.e., sandy soil). As part of the ongoing research project, the finished tests of free-field are mainly investigating the variation laws of subgrade reaction coefficient. Future research will focus on the soil-structure interaction through quasistatic test method; firstly the deformation of free-field should be calculated in advance according to three seismic fortification levels (i.e., frequent earthquakes, fortification earthquakes, and rare earthquakes); then, the free-field deformation will be applied to the lateral boundary of the soil by the pushover slide plate.

Data Availability

The data used to support the research of present study are available from the corresponding author upon request.

Conflicts of Interest

The authors declare that there are no conflicts of interest regarding the publication of this article.

Acknowledgments

The authors would like to acknowledge the support provided by the Scientific Research Fund of Institute of Engineering Mechanics, China Earthquake Administration (Grant no. 2017B10), the National Key Research and Development Program (Grant no. 2016YFC0800205), and the National Natural Science Foundation of China (Grant no. 51438004).

References

[1] Y. M. A. Hashash, J. J. Hook, B. Schmidt, and J. I-Chiang Yao, "Seismic design and analysis of underground structures," *Tunnelling and Underground Space Technology*, vol. 16, no. 4, pp. 247–293, 2001.

[2] K. Uenishi and S. Sakurai, "Characteristic of the vertical seismic waves associated with the 1995 Hyogo-ken Nanbu (Kobe), Japan earthquake estimated from the failure of the Daikai Underground Station," *Earthquake Engineering and Structural Dynamics*, vol. 29, no. 6, pp. 813–821, 2001.

[3] Y. Hayashi, K. Tamura, M. Mori, and I. Takahashi, "Simulation analyses of buildings damaged in the 1995 Kobe, Japan, earthquake considering soil-structure interaction," *Earthquake Engineering & Structural Dynamics*, vol. 28, no. 4, pp. 371–391, 1999.

[4] J. H. Wang, M. W. Huang, K. C. Chen, R. D. Hwang, and W. Y. Chang, "Aspects of characteristics of near-fault ground motions of the 1999 chi-chi (Taiwan) earthquake," *Journal of the Chinese Institute of Engineers*, vol. 25, no. 5, pp. 507–519, 2002.

[5] J. X. Lai, S. Y. He, J. L. Qiu et al., "Characteristics of seismic disasters and aseismic measures of tunnels in Wenchuan earthquake," *Environmental Earth Sciences*, vol. 76, no. 2, p. 94, 2017.

[6] B. Ruan, Y. Miao, K. Cheng, and E.-L. Yao, "Study on the small strain shear modulus of saturated sand-fines mixtures by bender element test," *European Journal of Environmental and Civil Engineering*, pp. 1–11, 2018.

[7] Y. Miao, E. Yao, B. Ruan, and H. Zhuang, "Seismic response of shield tunnel subjected to spatially varying earthquake ground motions," *Tunnelling and Underground Space Technology*, vol. 77, pp. 216–226, 2018.

[8] Y. Miao, E. Yao, B. Ruan, H. Zhuang, G. Chen, and X. Long, "Improved Hilbert spectral representation method and its application to seismic analysis of shield tunnel subjected to spatially correlated ground motions," *Soil Dynamics and Earthquake Engineering*, vol. 111, pp. 119–130, 2018.

[9] Z. Y. Chen, W. Y. Li, and L. D. Yang, "Simplified seismic design method for Shanghai underground structures in soft soils," *Indian Geotechnical Journal*, vol. 44, no. 2, pp. 149–155, 2014.

[10] W. Li and Q. Chen, "Seismic performance and failure mechanism of a subway station based on nonlinear finite element analysis," *KSCE Journal of Civil Engineering*, vol. 22, no. 2, pp. 765–776, 2017.

[11] N. M. Newmark, "Problems in wave propagation in soil and rock," in *Proceedings of the International Symposium on Wave Propagation and Dynamic Properties of Earth Materials*, pp. 7–26, New Mexico, Mexico, August 1968.

[12] J. Penzien, "Seismically induced racking of tunnel linings," *Earthquake Engineering & Structural Dynamics*, vol. 29, no. 5, pp. 683–691, 2000.

[13] J. N. Wang, *Seismic Design of Tunnels: A Simple State of the Art Design Approach*, Parsons Brinckerhoff Quade and Douglas Inc., New York, NY, USA, 1993.

[14] A. L. Sánchez-Merino, J. Fernández-Sáez, and C. Navarro, "Simplified longitudinal seismic response of tunnels linings subjected to surface waves," *Soil Dynamics and Earthquake Engineering*, vol. 29, no. 3, pp. 579–582, 2009.

[15] K. Kawashima, *The Seismic Design of Underground Structures*, Kashima Publishing, Tokyo, Japan, 1994.

[16] J. Liu, W. Wang, and G. Dasgupta, "Pushover analysis of underground structures: method and application," *Science China Technological Sciences*, vol. 57, no. 2, pp. 423–437, 2014.

[17] The National Standards Compilation Group of People's Republic of China, *Code for Seismic Design of Urban Rail Transit Structures (CNS GB50909-2014)*, China Architecture and Building Press, Beijing, China, 2014, in Chinese.

[18] The National Standards Compilation Group of People's Republic of China, *Code For Seismic Design of Buildings (CNS GB50011-2010)*, China Architecture and Building Press, Beijing, China, 2010, in Chinese.

[19] The National Standards Compilation Group of People's Republic of China, *Code for Seismic Design of Nuclear Power Plants (CNS GB50267-1997)*, Standards Press of China, Beijing, China, 1997, in Chinese.

[20] S. C. Dutta and R. Roy, "A critical review on idealization and modeling for interaction among soil–foundation–structure system," *Computers and Structures*, vol. 80, no. 20-21, pp. 1579–1594, 2002.

[21] K. Terzaghi, "Evalution of coefficients of subgrade reaction," *Géotechnique*, vol. 5, no. 4, pp. 297–326, 1955.

[22] A. Burhan and G. Ayhan, "Modulus of subgrade reaction that varies with magnitude of displacement of cohesionless soil," *Arabian Journal of Geosciences*, vol. 11, no. 13, pp. 351–358, 2018.

[23] P. S. Lin, L. W. Yang, and C. H. Juang, "Subgrade reaction and load-settlement characteristics of gravelly cobble deposits by plate-load tests," *Canadian Geotechnical Journal*, vol. 35, no. 5, pp. 801–810, 2011.

[24] Y. J. Choi, S. Lee, J. Oh, J. Ahn, and J. Jung, "Coefficient of subgrade reaction for the permeable block and base system at Korea GI and LID center," *Civil Infrastructures Confronting Severe Weathers and Climate Changes Conference*, pp. 69–75, Springer Publishing, Cham, Switzerland, 2018.

[25] M. Firuzi, E. Asghari-Kaljahi, and H. Akgün, "Correlations of SPT, CPT and pressuremeter test data in alluvial soils. Case study: Tabriz Metro Line 2, Iran," *Bulletin of Engineering Geology and the Environment*, vol. 78, no. 7, pp. 5067–5086, 2019.

[26] Y. T. Yu and H. Tang, "Reaction coefficient of subgrade on Xi'an loess and correlation analysis of methods of measurement," *Chinese Journal of Rock Mechanics and Engineering*, vol. 36, no. 10, pp. 2563–2571, 2017, in Chinese.

[27] Y. J. Pan, G. S. Li, S. C. Liu, T. J. Ouyang, and G. C. Cai, "Study on the test method and value of the horizontal subgrade coefficient," *Chinese Journal of Underground Space and Engineering*, vol. 14, no. 3, pp. 712–718, 2018, in Chinese.

[28] S. Yin, L. W. Kong, A. W. Yang, and K. Mu, "Indoor experimental study of road performance of granite residual soil for subgrade filling materials," *Rock and Soil Mechanics*, vol. 37, no. 2, pp. 287–293, 2016, in Chinese.

[29] C. M. S. John and T. F. Zahrah, "Aseismic design of underground structures," *Tunnelling and Underground Space Technology*, vol. 2, no. 2, pp. 165–197, 1987.

[30] H. F. Sun, L. P. Jing, X. C. Meng, and N. W. Wang, "A three-dimensional laminar shear soil container for shaking table test," *Journal of Vibration and Shock*, vol. 31, no. 17, pp. 26–32, 2012, in Chinese.

[31] M. Zeghal, A.-W. Elgamal, H. T. Tang, and J. C. Stepp, "Lotung downhole array. II: evaluation of soil nonlinear properties," *Journal of Geotechnical Engineering*, vol. 121, no. 4, pp. 363–378, 1995.

[32] The National Standards Compilation Group of People's Republic of China, *Code For Geotechnical Investigations of Urban Rail Transit (CNS GB50307-2012)*, China Planning Press, Beijing, China, 2012, in Chinese.

[33] A. Paparo and K. Beyer, "Quasi-static cyclic tests of two mixed reinforced concrete-unreinforced masonry wall structures," *Engineering Structures*, vol. 71, pp. 201–211, 2014.

[34] Z. G. Sun, D. S. Wang, T. Wang, S. W. Wu, and X. Guo, "Investigation on seismic behavior of bridge piers with thin-walled rectangular hollow section using quasi-static cyclic tests," *Engineering Structures*, vol. 200, Article ID 109708, 2019.

[35] M. T. Suleiman, L. Ni, A. Raich, J. Helm, and E. Ghazanfari, "Measured soil-structure interaction for concrete piles subjected to lateral loading," *Canadian Geotechnical Journal*, vol. 52, no. 8, pp. 1168–1179, 2015.

[36] J.-S. Chiou, Y.-Y. Ko, S.-Y. Hsu, and Y.-C. Tsai, "Testing and analysis of a laterally loaded bridge caisson foundation in gravel," *Soils and Foundations*, vol. 52, no. 3, pp. 562–573, 2012.